# Late Pliocene vegetation turnover on the NE Tibetan Plateau (Central Asia) triggered by early Northern Hemisphere glaciation

Andreas Koutsodendris[1*], Frederik J. Allstädt[1], Oliver A. Kern[1], Ilias Kousis[1], Florian Schwarz[2], Martina Vannacci[1], Amber Woutersen[3], Erwin Appel[4], Melissa A. Berke[5], Xiaomin Fang[6], Oliver Friedrich[1], Carina Hoorn[3], Ulrich Salzmann[2], Jörg Pross[1]

[1]Institute of Earth Sciences, Heidelberg University, 69120 Heidelberg, Germany
[2]Department of Geography and Environmental Sciences, Northumbria University, NE18ST, Newcastle upon Tyne, United Kingdom
[3]Institute for Biodiversity and Ecosystem Dynamics, University of Amsterdam, 1090 GE, Amsterdam, The Netherlands
[4]Department of Geosciences, University of Tübingen, 72074 Tübingen, Germany
[5]Department of Civil and Environmental Engineering & Earth Sciences, University of Notre Dame, 156 Fitzpatrick Hall, IN 46556, Notre Dame, USA
[6]Institute of Tibetan Plateau Research, Chinese Academy of Sciences, P.O. Box 2871, 100085, Beijing, China

* Correspondence to: Andreas Koutsodendris (andreas.koutsodendris@geow.uni-heidelberg.de)

## Abstract

To reconstruct the timing and underlying forcing of major shifts in the composition of terrestrial ecosystems in arid Central Asia during the late Cenozoic (past ~7 Ma), we carry out palynological analysis of lake sediments from the Qaidam Basin (NE

Tibetan Plateau, China). Our results show that the steppe/semi-desert biomes dominating the Qaidam Basin experienced marked turnovers at ~3.6 and 3.3 Ma. Most notably, the younger of these turnover events is characterized by a two- to three-fold expansion of *Artemisia* at the expense of other steppe/semi-desert taxa. This turnover event led to the replacement of the Ephedraceae/Chenopodiaceae-dominated and *Nitraria*-rich steppe/semi-deserts that were dominant in the Qaidam Basin during the Paleogene and abundant during the Miocene by *Artemisia*/Chenopodiaceae-dominated steppe/semi-deserts as they exist until today. The vegetation turnover events are synchronous with shifts towards drier conditions in Central Asia as documented in climate records from the Chinese Loess Plateau and the Central North Pacific Ocean. On a global scale, they can be correlated to early glaciation events in the Northern Hemisphere during the Pliocene. Integration of our palynological data from the Qaidam Basin with Northern Hemisphere climate-proxy and regional-scale tectonic information suggests that the uplift of the Tibetan Plateau posed ecological pressure on Central Asian plant communities, which made them susceptible to the effects of early Northern Hemisphere glaciations during the late Pliocene. Although these glaciations were relatively small in comparison to their Pleistocene counterparts, the transition towards drier/colder conditions pushed previously existing plant communities beyond their tolerance limits, thereby causing a fundamental reorganization of arid ecosystems. The *Artemisia* dominance since ~3.3 Ma resulting from this reorganization marks a point in time after which the *Artemisia*/Chenopodiaceae pollen ratio can serve as a reliable indicator for moisture availability in Central Asia.

**Keywords**

Aridification; Neogene; Northern Hemisphere glaciation; Qaidam Basin; Tibetan Plateau; vegetation dynamics

## 1. Introduction

As a result of anthropogenic climate change, considerable shifts in hydrological conditions are projected for Central Asia for the near future (IPCC, 2014). It is therefore crucial to obtain a better understanding of the climatic forcing on plant-community dynamics in the affected regions in order to extend the lead time for mitigation and adaptation. In this context, the study of past intervals in Earth history that were warmer than today and had atmospheric carbon dioxide concentrations ($pCO_2$) similar to those expected for the near future (Martínez-Botí et al., 2015; Burke et al., 2018) provides a promising avenue for predicting future developments. From late Miocene (~11.6–5.3 Ma) to Pliocene (~5.3–2.6 Ma) times, global temperatures were several degrees warmer and atmospheric $pCO_2$ was slightly higher than today (Burke et al., 2018; Holbourn et al., 2018). Thus, the late Neogene represents the most recent geological interval that can serve as an analogue for a future anthropogenic greenhouse world.

Central Asia was among the most arid regions on Earth during most of the Neogene and forms a key region for deciphering the evolution of ecosystems in arid environments (Guo et al., 2002; An et al., 2005; Dupont-Nivet et al., 2007). Changes in the carbon-isotope signatures of soils from the Chinese Loess Plateau during the past 7 Ma have documented a major shift in plant communities at ~3.6 Ma, associated with the expansion of drought-tolerant $C_4$ plants at the expense of plants exploiting the $C_3$ photosynthetic pathway (An et al., 2005). Palynological data are in agreement with these findings; they document that *Artemisia* emerged as the dominant taxon in arid regions across China during the late Pliocene (Wang, 2004; Miao et al., 2011b; Cai et al., 2012). This expansion occurred at the expense of Chenopodiaceae and other drought-tolerant taxa (e.g., Ephedraceae, *Nitraria*) that prevailed in Central Asia since the Paleogene (Hoorn et al., 2012; Han et al., 2016;

Miao et al., 2016). This shift in plant communities has been attributed predominantly to the uplift of the Tibetan Plateau and its impact on regional monsoonal dynamics (An et al., 2001; Molnar et al., 2010), but may also represent a response to global late Neogene cooling (Zhang et al., 2001; Guo et al., 2002; Lu et al., 2010; Licht et al., 2016). Because of the lack of continuous, highly resolved and well-dated vegetation records, the signature, timing and duration of these vegetation transitions, and, by extension, the underlying trigger mechanisms have remained poorly constrained.

We here present a new palynological record from drillcores that were retrieved from the Qaidam Basin (north-eastern Tibetan Plateau) and spans from ~7.3 until 0.1 Ma ago (Figure 1). To warrant detailed analysis of previously recognized phases of pronounced vegetation turnover in Central Asia, we have studied the mid-Pliocene to late Pleistocene interval in high (millennial- to suborbital-scale) temporal resolution (~3–4 ka). The remainder of the drillcore record was studied in orbital- to tectonic-scale resolution (~10 to >30 ka) in order to reconstruct the long-term vegetation development since the late Miocene. To better constrain the impacts of both the Tibetan Plateau uplift and global climate change on the evolution of plant communities in the Qaidam Basin, we compare our palynological data with supraregional terrestrial (e.g., Chinese Loess Plateau) and marine (e.g., North Pacific) climate-proxy records.

## 2. Regional setting

Situated close to the north-eastern margin of the Tibetan Plateau, the Qaidam Basin ranges among the highest, most evaporative, and largest inland basins of Central Asia (Fang et al., 2007; Yang et al., 2011). It lies at an average altitude of ~2800 m above sea level and is surrounded by up to ~5000 m high mountain ranges (Figure 1). Basin formation started in the early Eocene as a result of orogenic shortening due

to the India-Eurasia continental collision (Wang et al., 2008; Yin, 2010). Further expansion and deepening prevailed until the mid-Miocene (Fang et al., 2007), but from the late Miocene onwards tectonic compression led to shrinking of the basin (Wang et al., 2012; Yuan et al., 2013). Today, the basin hosts one of world's thickest fluvio-lacustrine Cenozoic sedimentary records, with a maximum thickness of ~15 km (Fang et al., 2007).

As most other regions of Central Asia, the Qaidam Basin has undergone gradual drying through the Cenozoic, with the Miocene being wetter than the Pliocene and Pleistocene, respectively (Wang et al., 1999; Fang et al., 2007). This drying has been attributed to a combination of tectonic activity in Central Asia, including the northward drift and uplift of the basin connected to Tibetan Plateau uplift, and global Cenozoic cooling (Wang et al., 1999; Fang et al., 2007). To date, the basin is characterized by a W–E precipitation gradient; for the western part of the basin where the study material comes from, mean annual precipitation is 15.8 mm and mean annual potential evaporation is 2967 mm (Lenghu meteorological station for the period 1957–2000; Chen et al., 2013).

Because of the prevailing (hyper)arid conditions, the modern vegetation in the Qaidam Basin represents a transition between the Mongolian desert and the alpine steppe of the Tibetan Plateau (Walter and Box, 1983). Specifically, four major biomes (i.e., alpine meadows, steppes, steppe/deserts, and deserts) occur in the Qaidam Basin and the surrounding mountains (Yu et al., 2001; Zhao and Herzschuh, 2009; Zhang et al., 2010); they consist predominantly of herbs and shrubs of the genera *Artemisia*, *Calligonum*, *Ephedra*, *Haloxylon*, *Kalidium*, *Nitraria*, *Reaumuria*, *Salsola*, *Sympegma*, and *Tamarix* (Zhao and Herzschuh, 2009; Zhao et al., 2007, 2010; Wei et al., 2011). Forests are confined to the surrounding mountains and mainly consist of *Betula, Pinus*, and *Picea* (Zhao et al., 2009; Wei et al., 2011).

## 3. Material and methods

Two long drillcores were recovered in 2008 and 2011 from paleolake sediments in the western Qaidam Basin (Figure 1). Core SG-1 (38˚24´35˝N, 92˚30´33˝E) was drilled in the depocenter of the Chahansilatu sub-basin to a depth of 938 m with a recovery of ~95 % (Zhang et al., 2012a). Core SG-1b (38˚21´9.46˝N, 92˚16´24.72˝E) was recovered from the Jianshan anticline, ~20 km SW of core SG-1, and reached a depth of 723 m; recovery is ~93 % with the exception of the topmost 60 m, where core loss was ~20 % (Zhang et al., 2014). Lithologically, both cores consist predominantly of lacustrine clay-, silt- and calcareous mudstones with intercalated marl, halite and gypsum layers (Figure 2; Wang et al., 2012; Zhang et al., 2012b; Lu et al., 2015).

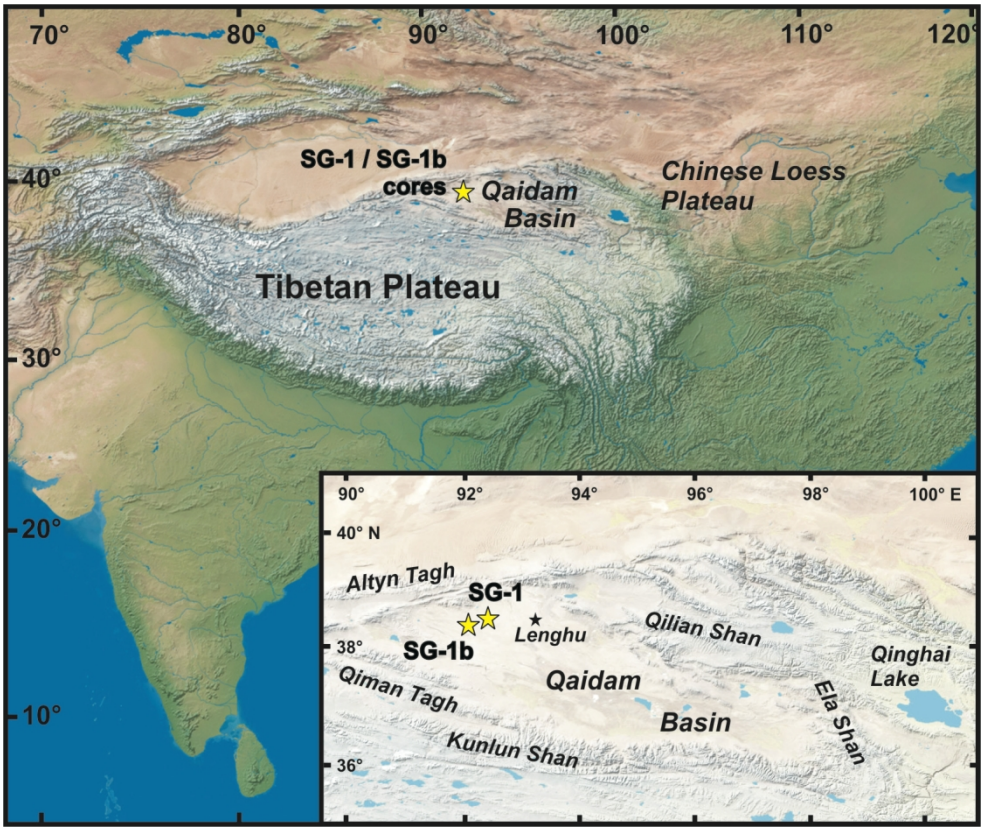


**Figure 1:** Locations of the SG-1 and SG-1b cores in Central Asia and within the Qaidam Basin (insert map).

155

156 **3.1 Chronology**

157 Age control for core SG-1 is based on the integration of magnetostratigraphy, optical
158 stimulated luminescence (OSL) and U-Th dating, and cyclostratigraphy. The
159 observed magnetic polarity zones were correlated with Chrons 1n-2An of the
160 geomagnetic polarity time scale (Zhang et al., 2012a). The age model was further
161 refined by cyclostratigraphic analysis of a high-resolution magnetic susceptibility
162 dataset yielding a basal age of 2.69 Ma (Herb et al., 2013; Herb et al., 2015a). The
163 core top has an OSL- and U/Th-based minimum age of ~77.8 ± 4.0 ka (Han et al.,
164 2014). The chronology of core SG-1b is based on magnetostratigraphy yielding a late
165 Miocene to early Pleistocene age (Chrons 2n-3Br; ~7.3 to 1.6 Ma; Zhang et al.,
166 2014). Based on their age models, the SG-1 and SG-1b cores overlap between ~2.6
167 and 1.6 Ma.

168

169 **3.2 Palynology**

170 In total, 847 pollen samples were analysed from both cores. Specifically, 505
171 samples were newly processed and counted for this study; this dataset was
172 augmented by another 342 samples previously published in Herb et al. (2015b) and
173 Koutsodendris et al. (2018). All samples were processed following standard
174 palynological techniques including freeze-drying, HCl (30 %) and HF (38 %)
175 digestion, treatment with KOH, heavy-liquid density separation, and sieving through a
176 10 μm mesh. At least 250 pollen grains were counted for 95 % of the samples
177 (mean: 333; range: 23–801 grains), excluding pollen from aquatic plants and spores.
178 For the calculation of pollen percentages, pollen from aquatic plants and fern spores
179 were excluded because they bear a strongly local vegetation signal. All palynological
180 plots were generated using the C2 software.

181

### 3.3 Statistical evaluation

Principal component analysis (PCA) was carried out using the PAST software to examine the relationships among the dominant pollen taxa in the core material. PCA was applied on a set of selected steppe/desert taxa that are continuously present in the record; arboreal and aquatic taxa were included in the analysis as groups.

## 4. Results

### 4.1 Palynological analysis of cores SG-1 and SG-1b

All palynological samples from cores SG-1 and SG-1b are dominated by herbaceous and shrubby taxa, particularly Chenopodiaceae (mean: 30 %; maximum: 51 %), *Artemisia* (28 % and 76 %), Poaceae (12 % and 40 %), Ephedraceae (5 % and 39 %), Cyperaceae (5 % and 25 %), and Asteraceae (4 % and 16 %) (Figure 2). Several other herbs and shrubs with average abundances <1 % are present continuously across the study interval; some of these taxa transiently reach higher abundances, such as Tamaricaceae (maximum: 13 %), Elaeagnaceae (12 %), Ranunculaceae (11 %), *Calligonum* (7 %), Caryophyllaceae (7 %), and *Nitraria* (6 %).

Arboreal pollen (AP) represent only a small percentage of the pollen sum, with conifers and broad-leaved deciduous trees on average making up for 5 and 2 % of the assemblages, respectively (Figure 2). The main conifer taxa include *Pinus* (maximum: 54 %), Cupressaceae (13 %), *Picea* (13 %), and *Abies* (3 %); *Cedrus*, *Larix*, *Podocarpus*, and *Tsuga* occur in low amounts. The most common deciduous broad-leaved trees comprise *Betula* (maximum: 9 %), *Ulmus* (7 %), *Alnus* (5 %), *Quercus* (4 %), and *Juglans* (3 %); low amounts of *Carpinus, Corylus, Fraxinus, Salix,* and *Tilia* were also registered. Finally, aquatic plants including *Typha latifolia*, *T. angustifolia,* and *Potamogeton* are continuously present, with average abundances of 3 % (maximum: 22 %) (Figure 2).

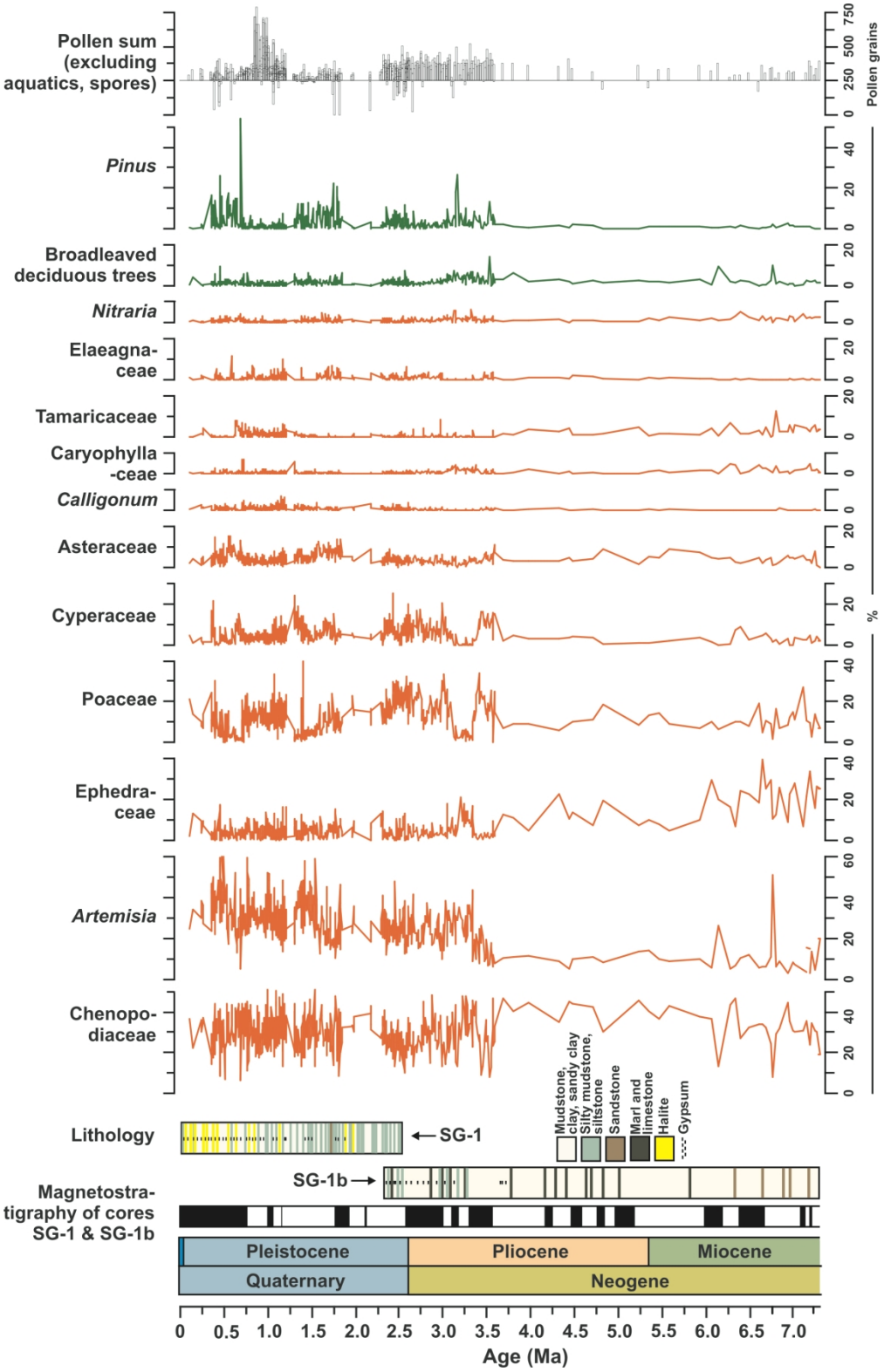


208

209 **Figure 2:** Pollen percentages of selected pollen taxa identified in the SG-1 and SG-
210 1b cores spanning the past 7.3 Ma. Magnetostratigraphy and cores lithologies are
211 adapted from Wang et al. (2012), Zhang et al. (2012b, 2014) and Lu et al. (2015).

While the spectrum of pollen-producing plants has remained remarkably stable in the Qaidam Basin since the late Miocene, closer inspection reveals substantial changes in the abundances of the dominant taxa. Whereas Chenopodiaceae percentages remained rather stable throughout the record (~30 %), the percentages of other dominant taxa such as *Artemisia,* Ephedraceae and Poaceae exhibit considerable variability (Figure 2). Specifically, *Artemisia* abundances increased from an average of 12 % (~7.3 –3.3 Ma) to 30 % (~3.3–0.3 Ma), and Ephedraceae abundances decreased from an average of 18 % (~7.3–3.7 Ma) to 4 % (~3.7–0.3 Ma). In addition, Poaceae abundances show a quasi-cyclical behaviour with high values of 19–20 % on average during ~3.5–3.3 and ~3.1–2.3 Ma, and 14 % during ~1.2–0.7 Ma; instead, values <5 % occurred during ~3.3–3.1, 1.6–1.3, and 0.7–0.6 Ma (Figure 2). Among the arboreal taxa, the percentages of *Pinus* increased from ~3.6 Ma onwards at the expense of all other tree-pollen taxa (including deciduous trees and conifers other than *Pinus*) (Figure 2).

### 4.2 Principal component analysis

The PCA yields three major components that account for 80.2 % of the total variance of our pollen dataset (Table 1). The first component explains 38.4 % of the total variance and is bipolar; it is primarily driven by *Artemisia*, which is marked by highly negative loadings, and Poaceae, Chenopodiaceae and AP, which are characterized by positive loadings (Table 2; Figure 3). The second component is also bipolar and explains 27.4 % of the total variance. Whereas its negative pole is primarily driven by Chenopodiaceae and to a lesser extent by Ephedraceae, its positive pole is driven by Poaceae and AP. The third component, which explains 14.4 % of the total variance, is also bipolar (Tables 1 and 2). It is marked by highly positive loadings of AP and highly negative loadings of Poaceae.

239 **Table 1:** Total variance explained by the first three PCA components of the pollen
240 dataset from the SG-1 and SG-1b cores.

| PC | Eigenvalue | % variance |
|---|---|---|
| 1 | 115.245 | 38.4 |
| 2 | 82.2967 | 27.4 |
| 3 | 43.0543 | 14.4 |

241

242 **Table 2:** PCA loadings of the pollen dataset from the SG-1 and SG-1b cores.

| | PC 1 | PC 2 | PC 3 |
|---|---|---|---|
| Arboreal pollen (AP) | **0,168** | **0,364** | **0,675** |
| Elaeagnaceae | 0,024 | 0,035 | -0,019 |
| Tamaricaceae | 0,022 | -0,045 | -0,006 |
| Ephedraceae | 0,049 | **-0,132** | **0,143** |
| *Artemisia* | **-0,901** | 0,039 | **-0,125** |
| Chenopodiaceae | **0,210** | **-0,800** | -0,078 |
| Apiaceae | 0,002 | -0,005 | -0,004 |
| Brassicaceae | 0,006 | -0,008 | -0,012 |
| *Calligonum* | -0,011 | -0,010 | -0,034 |
| Caryophyllaceae | 0,011 | -0,012 | 0,022 |
| Asteraceae | 0,014 | 0,027 | **0,134** |
| Cyperaceae | 0,078 | **0,160** | 0,033 |
| Poaceae | **0,321** | **0,423** | **-0,693** |
| Rosaceae | 0,009 | 0,003 | -0,005 |
| *Thalictrum* | -0,001 | 0,004 | 0,011 |
| Aquatics | 0,058 | 0,003 | 0,028 |

243

## 5. Discussion

### 5.1 Timing and causes of major vegetation turnover in the Qaidam Basin

Our palynological data from cores SG-1 and SG-1b document that a steppe/semi-desert biome dominated the vegetation in the Qaidam Basin from the late Miocene to the late Pleistocene (Figure 2). The PCA results show that the distribution of the dominant taxa is controlled by different factors. The first PCA component primarily differentiates *Artemisia* from Chenopodiaceae and Ephedraceae, whereas the second component differentiates the latter taxa from Poaceae and AP (Figure 3). Moreover, the third component further differentiates Poaceae from AP. Considering the modern distribution of these taxa in the Qaidam Basin (Zhao et al., 2007, 2009; Zhao and Herzschuh, 2009), we explain the first two components to represent the differentiation between *Artemisia*- and Chenopodiaceae/Ephedraceae-dominated steppe/semi-deserts. By extension, the third component differentiates between local and distal pollen sources, considering that grasses predominantly grow in proximity to the lake shores in the Qaidam Basin whereas forests develop only in the surrounding mountains (Cour et al., 1999; Zhao et al., 2007, 2009; Wei et al., 2011).

A closer look reveals a series of changes in the composition of the steppe/semi-desert vegetation during the late Pliocene. A first vegetation turnover at ~3.6 Ma is characterized by an increase in *Artemisia*, Poaceae and Cyperaceae abundances, and a coeval decrease in Ephedraceae and Chenopodiaceae abundances (Figure 2). A second, fundamental turnover in the composition of the steppe/desert vegetation in the Qaidam Basin occurred at ~3.3 Ma. It is marked by a two- to three-fold increase in *Artemisia* percentages at the expense of other steppe/desert taxa including Ephedraceae, Asteraceae and Tamaricaceae (Figure 2). This interval is also marked by a shift in the composition of the forests that thrived on the mountain slopes surrounding the Qaidam Basin; the abundance of the cold- and drought-tolerant *Pinus* increased at the expense of warmth- and high-moisture-demanding

deciduous trees (Figure 2). These two abrupt turnover events refine the exact timing of the *Artemisia* expansion in the Qaidam Basin. Based on the neighbouring pollen records from cores SG3 and KC-1 from the western Qaidam Basin that discontinuously span the past 18 Ma, this expansion can be placed between 5 and 3 Ma (Miao et al., 2011a; Cai et al., 2012).

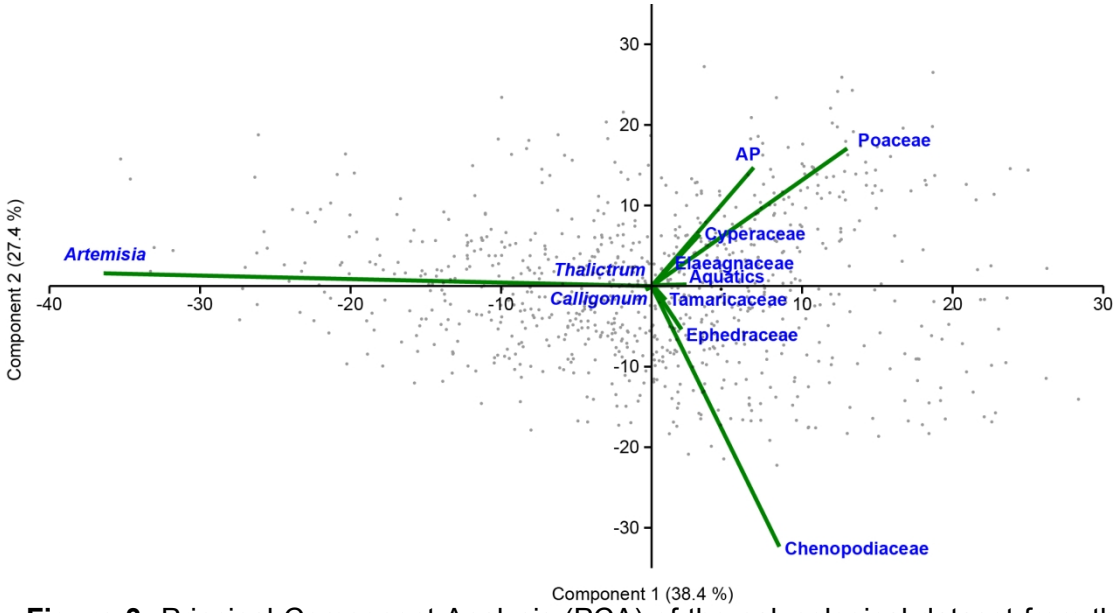


**Figure 3:** Principal Component Analysis (PCA) of the palynological dataset from the SG-1 and SG-1b cores. The first two components explain 65.8 % of the total variance.

The vegetation-turnover events coincide with sedimentological and geochemical changes in core SG-1b and suggest two major climate shifts at ~3.6 and ~3.3 Ma, respectively. Increases in the medium-coarse silt and sand fractions in the respective core intervals indicate lake-level drops, and by extension, a prevalence of drier conditions (Lu et al., 2015). This finding is further supported by the coeval deposition of evaporites in the SG-1b core (Fang et al., 2016). On a supraregional scale, synchronous transitions towards drier conditions in Central Asia are also documented for the Chinese Loess Plateau and the Pacific Ocean. On the Chinese

289 Loess Plateau, an increase in the size of quartz grains in the loess deposits at ~3.6
290 Ma indicates enhanced wind strength resulting from a stronger influence of the cold
291 and dry air masses of the winter monsoon (An et al., 2001; Lu et al., 2010). The
292 coeval increase of $C_4$ plants on the Chinese Loess Plateau also suggests a shift in
293 plant communities in response to a stronger prevalence of dry conditions (An et al.,
294 2005). The onset of drier conditions at ~3.6 Ma is further evidenced by enhanced
295 dust delivery from Central Asia into the Central Pacific Ocean as documented at
296 Ocean Drilling Program (ODP) Sites 885 and 886 (Rea et al., 1998; Figure 4). This
297 pattern is coeval with the *Artemisia* percentage increase in the SG-1 and SG-1b
298 cores from the Qaidam Basin (Figure 4).

299 Because *Artemisia* requires a higher moisture availability than Chenopodiaceae and
300 Ephedraceae during the growing season (El'Moslimany, 1990; Cour et al., 1999), its
301 expansion at the expense of other drought-tolerant steppe/semi-desert taxa against a
302 background of an increasingly dry climate during the late Pliocene (Rea et al., 1998;
303 An et al., 2001; Lu et al., 2010; Sun et al., 2010) cannot be explained by a
304 prevalence of wetter conditions. Instead, it could be plausibly explained through a
305 seasonal shift in moisture availability. Quantitative analysis of the annual distribution
306 of modern pollen rain along the western border of the Qaidam Basin has shown that
307 maximum abundances of *Artemisia* pollen occur in late summer and autumn; in
308 contrast, maxima in Chenopodiaceae, Ephedraceae, Poaceae, and Tamaricaceae
309 pollen abundances occur in early summer (Cour et al., 1999). This pattern suggests
310 that the late Pliocene expansion of *Artemisia* could result from a seasonal shift of
311 maximum precipitation from summer to autumn, with the shift in moisture availability
312 giving the taxon a competitive advantage over Chenopodiaceae and Ephedraceae.
313 Support for such a scenario comes from the decoupling of the winter and summer
314 monsoon systems as evidenced in sedimentological data from the Chinese Loess
315 Plateau (Sun et al., 2010). Whereas the Miocene and early Pliocene climates in

Central Asia were characterized by enhanced summer precipitation, late Pliocene and Pleistocene climates were marked by relatively low summer precipitation (Sun et al., 2010). These findings further support our hypothesis that a seasonal shift in precipitation distribution caused the vegetation turnover in the Qaidam Basin and, by extension, in Central Asia during the late Pliocene.

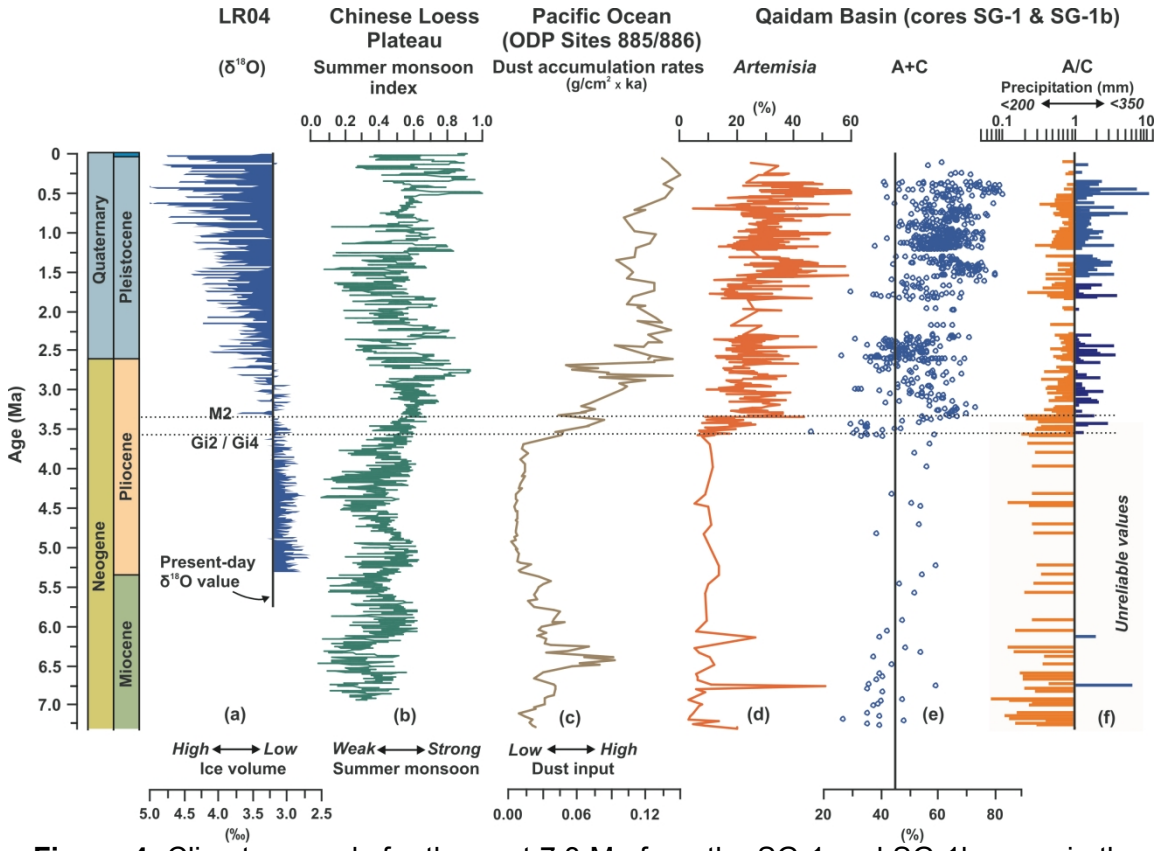


**Figure 4:** Climate records for the past 7.3 Ma from the SG-1 and SG-1b cores in the Qaidam Basin plotted against regional and global climate records. (a) LR04 global marine isotope stack (Lisiecki and Raymo, 2005); (b) East Asian summer monsoon index from the Lingtai section, Chinese Loess Plateau (Sun et al., 2010); (c) Dust accumulation rates at ODP Sites 885 and 886 in the North Pacific Ocean (Rea et al., 1998); (d) *Artemisia* pollen percentages, (e) sum of *Artemisia* and Chenopodiaceae (A+C) pollen percentages, and (f) *Artemisia*/Chenopodiaceae (A/C) ratio, in the SG-1 and SG-1b cores (this study). The A/C ratio is plotted against the 200 mm boundary for annual precipitation on the Tibetan Plateau as defined by an A/C value of 1 (Zhao et al., 2012). Turnover events are indicated with dashed lines.

331 The monsoonal variability in Central Asia since the Miocene has been predominantly
332 attributed to the tectonic uplift of the Tibetan Plateau (An et al., 2001), which poses a
333 physical obstacle to atmospheric flow and alters the temperature and pressure field
334 immediately above it due to surface heating (see Molnar et al., 2010, for a review).
335 Previous work has repeatedly invoked the increase in aridity (Rea et al., 1998; An et
336 al., 2001; Sun et al., 2010) and the expansion of drought-tolerant plants in Central
337 Asia (An et al., 2005) to Tibetan Plateau uplift. However, longer-term and gradual
338 tectonic forcing appears unlikely to have caused the rather abrupt shifts at ~3.6 and
339 ~3.3 Ma as evidenced in the palynological data from the Qaidam Basin. This is even
340 more so considering that the Qaidam Basin and surrounding mountain ranges had
341 reached elevations close to today already in the mid-Miocene (Wang et al., 2008;
342 Yuan et al., 2013). Hence, the abrupt shifts in steppe/desert composition as
343 documented by the *Artemisia* expansions at ~3.6 and ~3.3 Ma must have been
344 caused by a factor other than Tibetan Plateau uplift.

345 Conspicuously, both vegetation turnover events in the Qaidam Basin coincide with
346 the first major Northern Hemisphere glaciations of the Pliocene (de Schepper et al.,
347 2014). Specifically, the turnover at ~3.6 Ma occurs synchronously with the onset of
348 gradual cooling in the Northern Hemisphere as documented in a surface-water
349 temperature decline in the North Atlantic (Lawrence et al., 2009; Naafs et al., 2010)
350 and an ice-sheet expansion in the Arctic (de Schepper et al., 2014). Although the
351 glaciation at ~3.6 Ma is not linked to a specific marine isotope stage (MIS), it is highly
352 likely that it occurred during the Gi2 and/or Gi4 glacials (de Schepper et al., 2014).
353 The turnover in plant communities at ~3.3 Ma as documented by our palynological
354 data coincides with MIS M2, which stands out as the first glacial of the Pliocene
355 when local glaciers and ice caps in the Northern Hemisphere merged to modern-like
356 ice sheets (de Schepper et al., 2014). A quasi-global temperature decrease during
357 the M2 glaciation is documented for both the terrestrial and marine realms. Evidence

for such a cooling includes a surface-temperature drop (Naafs et al., 2010) and the deposition of ice-rafted debris (Kleiven et al., 2002) in the North Atlantic, a global sea-level drop of at least 10 m (Naish and Wilson, 2009), and an expansion of tundra vegetation at the expense of forests in Arctic Siberia associated with a ~5 °C decrease in the mean temperature of the warmest month (Brigham-Grette et al., 2013). Collectively, the timing and short duration of the vegetation shifts in the Qaidam Basin support the view that early Northern Hemisphere glaciations during the Pliocene were responsible for the reorganization of vegetation communities in Central Asia. The cooler conditions resulting from cryosphere expansion in the high latitudes of the Northern Hemisphere (de Schepper et al., 2014) would have strengthened the Siberian High pressure system, thereby leading to colder and more arid conditions on the Tibetan Plateau (An et al., 2001; Sun et al., 2010).

Our data indicate unequivocally that the fundamental change in Central Asian vegetation substantially pre-dates the intensification of Northern Hemisphere glaciation during the Plio/Pleistocene transition at ~2.6 Ma (Naafs et al., 2012; de Schepper et al., 2014). It appears that the early glaciations of the late Pliocene, particularly the M2 glaciation, pushed previously existing plant communities beyond their tolerance limits. Notably, these glaciations were able to do so although they were markedly less pronounced than their Pleistocene counterparts (Lawrence et al., 2009; Naafs et al., 2012). The subsequent Pleistocene glaciations have only decreased the vegetation cover and led to changes in the proportion of the dominant taxa percentages without triggering any large-scale vegetation turnover (Koutsodendris et al., 2018). We attribute this apparent discrepancy to the ecological pressure that the uplift of the Tibetan Plateau since the late Miocene has exerted on these plant communities, notably via changes in monsoon dynamics associated with uplift (An et al., 2001; Sun et al., 2010). This ecological pressure made them susceptible to the climate perturbations connected to the first Northern Hemisphere

385 glaciations, even if those were of relatively small magnitude only. Our findings from
386 the Qaidam Basin support the view that terrestrial ecosystem changes in Central
387 Asia were primarily the result of global climate change rather than Tibetan Plateau
388 uplift (Zhang et al., 2001; Guo et al., 2002; Lu et al., 2010).

389

390 **5.2 Implications for the *Artemisia*/Chenopodiaceae ratio as a moisture indicator**

391 Because *Artemisia* requires more humidity during the growing season than
392 Chenopodiaceae, the *Artemisia*/Chenopodiaceae (A/C) ratio has long been used as
393 a qualitative index for moisture availability in arid regions during the past decades. In
394 this ratio, high (low) A/C values indicate wetter (drier) conditions (El-Moslimani, 1990;
395 van Campo and Gasse, 1993, Cour et al., 1999). This notion has been confirmed
396 repeatedly by the coupling of modern palynological and meteorological data across
397 the Tibetan Plateau that have yielded increasing A/C values from desert to steppe
398 environments and a positive correlation with annual precipitation (Herzschuh, 2007;
399 Zhao et al., 2012; Ma et al., 2017). By extension, the A/C ratio has been used to
400 reconstruct changes between steppe and desert biomes (Herzschuh et al., 2004; Luo
401 et al., 2009; Zhao and Herzschuh, 2009; Wei et al., 2011), and to infer semi-
402 quantitative information on annual precipitation (Zhao et al., 2012).

403 The suitability of the A/C ratio for the semi-quantitative reconstruction of moisture
404 availability has also led to its application to fossil pollen records from arid regions.
405 This holds particularly true for the Tibetan Plateau, where the A/C ratio has been
406 used in various studies spanning the Holocene (van Campo and Gasse, 1993; Zhang
407 et al., 2010; Zhao et al., 2007, 2010; Chen et al., 2013). According to Zhao et al.
408 (2012), the A/C ratio provides reliable semi-quantitative estimates for the moisture
409 variability in steppe/desert environments during the Holocene if (i) annual
410 precipitation is <500 mm and (ii) the sum of *Artemisia* and Chenopodiaceae (A+C)
411 pollen grains exceeds ~45 % of the total pollen sum. In a number of studies, the A/C

412 ratio has also been applied to pre-Holocene pollen assemblages, such as the
413 Pleistocene (Herb et al., 2015; Koutsodendris et al., 2018), Pliocene (Wang et al.,
414 2006; Cai et al., 2012), and Miocene (Hao et al., 2012a).

415 Considering the marked differences in *Artemisia* and Chenopodiaceae abundances
416 within Central Asian pollen assemblages since the Miocene (Miao et al., 2011a,b;
417 Cai et al., 2012; Figure 2) and their differences in water demand regarding seasonal
418 precipitation distribution (El'Moslimany, 1990; Cour et al., 1999), the question arises
419 since when the A/C ratio in Central Asian pollen records provides reliable estimates
420 for moisture availability. To answer this question, we apply the criteria of Zhao et al.
421 (2012) in their investigation of the A/C signal and its fidelity based on modern pollen
422 datasets from the Tibetan and Chinese Loess Plateaus on our pollen datasets from
423 the Qaidam Basin. The A+C percentages in our samples from the SG-1 and SG-1b
424 cores are consistently >45 % since the late Miocene (~6 Ma) (Figure 4), suggesting
425 that the A/C ratio may be used as a regional moisture indicator from that time
426 onwards. However, the A/C ratios remain consistently below 1 in all samples
427 between ~6 and ~3.6 Ma (Figure 4). Taken at face value, the A/C ratio would hence
428 suggest continually dry conditions for the late Miocene and early Pliocene. However,
429 this inference would contradict a large set of proxy information from Central Asia that
430 consistently document more humid conditions during that time than during the late
431 Pliocene and Pleistocene (An et al., 2001, 2005; Sun et al., 2010). Hence, the A/C
432 ratio on pollen data from the Qaidam Basin most likely yields erroneous results for
433 samples older than ~3.3 Ma. This can be attributed to the fact that the pollen
434 assemblages, although containing both *Artemisia* and Chenopodiaceae, were
435 dominated by Chenopodiaceae pollen (~35 % on average), with *Artemisia* pollen
436 typically occurring in low numbers only (~12 %; Figure 2). By extension, the A/C ratio
437 should be applied to fossil pollen spectra of the Qaidam Basin only after the strong
438 expansion of *Artemisia* at ~3.3 Ma.

The A/C values in the Qaidam Basin for the past 3.3 Ma show a cyclical behaviour that allows us to distinguish between drier and wetter intervals (Figure 4). These intervals broadly correlate with glacial–interglacial variability evidenced in sedimentological and biomarker data in core SG-1 during the Pleistocene (Koutsodendris et al., 2018), which is driven by the interplay of the summer and winter monsoon systems (An et al., 2001; Guo et al., 2009; Sun et al., 2010). Interestingly, the A/C maxima show an increasing trend throughout the late Pliocene/Pleistocene, with peak values during the mid-Pleistocene (Figure 4). This is in concert with climate reconstructions from the Chinese Loess Plateau, which document a gradually increasing influence of the Central Asian summer monsoon towards the youngest Pleistocene interglacials (An et al., 2001; Sun et al., 2010). Most notably, the A/C peak at ~0.5 Ma in the Qaidam Basin falls within MIS 13. This interglacial stands out as a time when a maximum in the summer monsoon coincided with a minimum in the winter monsoon, resulting in the lowest inland aridity in Central Asia for the entire Pleistocene (Guo et al., 2009; Hao et al., 2012b). The excellent agreement between our data from the Qaidam Basin and independent proxy records from the Chinese Loess Plateau suggest that the A/C ratio can be applied with high confidence as an indicator for moisture availability in arid Central Asia after the establishment of *Artemisia*/Chenopodiaceae-dominated steppe/deserts at ~3.3 Ma.

## 6. Conclusions

A new, continuous pollen and spore record has been generated from drillcore material from the western Qaidam Basin (NE Tibetan Plateau), allowing insights into the timing and underlying forcing of major shifts in vegetation composition of Central Asia during the past ~7 Ma. We find that the terrestrial ecosystems experienced a fundamental turnover during the late Pliocene associated with the establishment of *Artemisia*/Chenopodiaceae-dominated steppe/semi-desert biomes that exist until

today. Comparison with regional terrestrial and marine records strongly suggests that this vegetation shift was synchronous with the onset of drier conditions in Central Asia as a response to Tibetan Plateau uplift and the expansion of ice sheets in the high latitudes of the Northern Hemisphere shortly before the Plio/Pleistocene transition. Most notably, the strong expansion of *Artemisia* at ~3.6 and ~3.3 Ma at the expense of other steppe/semi-desert taxa coincides with the first glacials of the Pliocene. This suggests that plant communities in Central Asia were highly susceptible to the effects of the early Northern Hemisphere glaciations although the extent of these glaciations was relatively small when compared to their Pleistocene counterparts.

**Acknowledgements**

Christian Herb, Stefanie Kaboth, Yin Lu, and Weilin Zhang are thanked for discussions. This research received financial support from the German Ministry for Education and Research (BMBF) through the 'CAME II' project (grant 03G086B to JP), and the German Research Foundation (DFG) through grants FR2544/13 to OF, KO4960/4 to AK, and PR651/8 to JP.

**References**

An, Z., Kutzbach, J., Prell, W. L., & Porter, S. C. (2001). Evolution of Asian monsoons and phased uplift of the Himalaya-Tibetan plateau since Late Miocene times. *Nature, 411*, 62-66. doi.org/10.1038/35075035

An, Z., Huang, Y., Liu, W., Guo, Z., Clemens, S., Li, L., Prell, W., Ning, Y., Cai, Y., Zhou, W., Lin, B., Zhang, Q., Cao, Y., Qiang, X., Chang, H., & Wu, Z. (2005). Multiple expansions of C4 plant biomass in East Asia since 7 Ma coupled with strengthened monsoon circulation. *Geology, 33*(9), 705. doi:10.1130/g21423.1

492 Brigham-Grette, J., Melles, M., Minyuk, P., Andreev, A., Tarasov, P., DeConto, R.,
493 Koenig, S., Nowaczyk, N., Wennrich, V., Rosen, P., Haltia, E., Cook, T., Gebhardt,
494 C., Meyer-Jacob, C., Snyder, J., & Herzschuh, U. (2013). Pliocene warmth, polar
495 amplification, and stepped Pleistocene cooling recorded in NE Arctic Russia.
496 *Science, 340*(6139), 1421-1427. doi:10.1126/science.1233137

497 Burke, K. D., Williams, J. W., Chandler, M. A., Haywood, A. M., Lunt, D. J., & Otto-
498 Bliesner, B. L. (2018). Pliocene and Eocene provide best analogs for near-future
499 climates. *Proceedings of the National Academy of Sciences.*
500 doi.org/10.5061/dryad.0j18k00

501 Cai, M., Fang, X., Wu, F., Miao, Y., & Appel, E. (2012). Pliocene–Pleistocene
502 stepwise drying of Central Asia: Evidence from paleomagnetism and sporopollen
503 record of the deep borehole SG-3 in the western Qaidam Basin, NE Tibetan
504 Plateau. *Global and Planetary Change, 94-95*, 72-81.
505 doi:10.1016/j.gloplacha.2012.07.002

506 Chen, F., Qiang, M., Zhou, A., Xiao, S., Chen, J., & Sun, D. (2013). A 2000-year dust
507 storm record from Lake Sugan in the dust source area of arid China. *Journal of*
508 *Geophysical Research: Atmospheres, 118*(5), 2149-2160. doi:10.1002/jgrd.50140

509 Cour, P., Zheng, Z., Duzer, D., Calleja, M., & Yao, Z. (1999). Vegetational and
510 climatic significance of modern pollen rain in northwestern Tibet. *Review of*
511 *Palaebotany and Palynology, 104*, 183-204.

512 de Schepper, S., Gibbard, P. L., Salzmann, U., & Ehlers, J. (2014). A global
513 synthesis of the marine and terrestrial evidence for glaciation during the Pliocene
514 Epoch. *Earth-Science Reviews, 135*, 83-102. doi:10.1016/j.earscirev.2014.04.003

515 Dupont-Nivet, G., Krijgsman, W., Langereis, C. G., Abels, H. A., Dai, S., & Fang, X.
516 (2007). Tibetan plateau aridification linked to global cooling at the Eocene-
517 Oligocene transition. *Nature, 445*(7128), 635-638. doi:10.1038/nature05516

518 Fang, X., Zhang, W., Meng, Q., Gao, J., Wang, X., King, J., Song, C., Dai, S., &
519 Miao, Y. (2007). High-resolution magnetostratigraphy of the Neogene Huaitoutala
520 section in the eastern Qaidam Basin on the NE Tibetan Plateau, Qinghai
521 Province, China and its implication on tectonic uplift of the NE Tibetan Plateau.
522 *Earth and Planetary Science Letters, 258*(1-2), 293-306.
523 doi:10.1016/j.epsl.2007.03.042

524 Fang, X., Li, M., Wang, Z., Wang, J., Li, J., Liu, X., & Zan, J. (2016). Oscillation of
525 mineral compositions in Core SG-1b, western Qaidam Basin, NE Tibetan Plateau.
526 *Scientific Reports, 6*, 32848. doi:10.1038/srep32848

527 Guo, Z. T., Ruddiman, W. F., Hao, Q. Z., Wu, H. B., Qiao, Y. S., Zhu, R. X., Peng, S.
528 Z., Wie, J. J., Yuan, B. Y., & Liu, T. S. (2002). Onset of Asian desertification by 22
529 Myr ago inferred from loess deposits in China. *Nature*, *416*(6877), 159.
530 doi.org/10.1038/416159a

531 Guo, Z. T., Berger, A., Yin, Q. Z., & Qin, L. (2009). Strong asymmetry of hemispheric
532 climates during MIS-13 inferred from correlating China loess and Antarctica ice
533 records. *Climate of the Past*, *5*(1), 21-31. doi.org/10.5194/cp-5-21-2009

534 Han, W., Ma, Z., Lai, Z., Appel, E., Fang, X., & Yu, L. (2014). Wind erosion on the
535 north-eastern Tibetan Plateau: constraints from OSL and U-Th dating of playa salt
536 crust in the Qaidam Basin. *Earth Surface Processes and Landforms, 39*(6), 779-
537 789. doi:10.1002/esp.3483

538 Han, F., Rydin, C., Bolinder, K., Dupont-Nivet, G., Abels, H. A., Koutsodendris, A.,
539 Zhang, K., & Hoorn, C. (2016). Steppe development on the Northern Tibetan
540 Plateau inferred from Paleogene ephedroid pollen. *Grana, 55*(1), 71-100.
541 doi:10.1080/00173134.2015.1120343

542 Hao, H., Ferguson, D. K., Chang, H., & Li, C. S. (2012a). Vegetation and climate of
543 the Lop Nur area, China, during the past 7 million years. *Climatic change*, *113*(2),
544 323-338. doi.org/10.1007/s10584-011-0347-7

545 Hao, Q., Wang, L., Oldfield, F., Peng, S., Qin, L., Song, Y., Xu, B., Qiao, Y.,
546 Bloemendal, J., & Guo, Z. (2012b). Delayed build-up of Arctic ice sheets during
547 400,000-year minima in insolation variability. *Nature, 490*(7420), 393-396.
548 doi:10.1038/nature11493

549 Herb, C., Zhang, W., Koutsodendris, A., Appel, E., Fang, X., & Pross, J. (2013).
550 Environmental implications of the magnetic record in Pleistocene lacustrine
551 sediments of the Qaidam Basin, NE Tibetan Plateau. *Quaternary International,*
552 *313-314*, 218-229. doi:10.1016/j.quaint.2013.06.015

553 Herb, C., Appel, E., Voigt, S., Koutsodendris, A., Pross, J., Zhang, W., & Fang, X.
554 (2015a). Orbitally tuned age model for the late Pliocene-Pleistocene lacustrine
555 succession of drill core SG-1 from the western Qaidam Basin (NE Tibetan
556 Plateau). *Geophysical Journal International, 200*(1), 35-51. doi:10.1093/gji/ggu372

557 Herb, C., Koutsodendris, A., Zhang, W., Appel, E., Fang, X., Voigt, S., & Pross, J.
558 (2015b). Late Plio-Pleistocene humidity fluctuations in the western Qaidam Basin
559 (NE Tibetan Plateau) revealed by an integrated magnetic–palynological record
560 from lacustrine sediments. *Quaternary Research, 84*(3), 457-466.
561 doi:10.1016/j.yqres.2015.09.009

562 Herzschuh, U., Tarasov, P., Wünnemann, B., Hartmann, K., 2004. Holocene
563 vegetation and climate of the Alashan Plateau, NW China, reconstructed from
564 pollen data. Palaeogeography, Palaeoclimatology, Palaeoecology 211, 1-17. doi:
565 10.1016/j.palaeo.2004.04.001

566 Herzschuh, U. (2007). Reliability of pollen ratios for environmental reconstructions on
567 the Tibetan Plateau. *Journal of Biogeography, 34*(7), 1265-1273.
568 doi:10.1111/j.1365-2699.2006.01680.x

569 Holburn, A. E., Kuhnt, W., Clemens, S. C., Kochhann, K. G. D., Jöhnck, J., Lübbers,
570 L., & Andersen, N. (2018). Late Miocene climate cooling and intensification of
571 southeast Asian winter monsoon. *Nature Communications, 9,* 1584.
572 doi.org/10.1038/s41467-018-03950-1

573 Hoorn, C., Straathof, J., Abels, H. A., Xu, Y., Utescher, T., & Dupont-Nivet, G.
574 (2012). A late Eocene palynological record of climate change and Tibetan Plateau
575 uplift (Xining Basin, China). *Palaeogeography, Palaeoclimatology, Palaeoecology,*
576 *344-345*, 16-38. doi:10.1016/j.palaeo.2012.05.011

577 IPCC (2014). Climate change 2014: Impacts, adaptation, and vulnerability. Part B:
578 Regional aspects. In V. R. Barros, C. B. Field, D. J. Dokken, M. D. Mastrandrea,
579 K. J. Mach, T. E. Bilir, M. Chatterjee, K. L. Ebi, Y. O. Estrada, R. C. Genova, B.
580 Girma, E. S. Kissel, A. N. Levy, S. MacCracken, P. R. Mastrandrea & L. L. White
581 (Eds.), Contribution of working group II to the fifth assessment report of the
582 intergovernmental panel on climate change. Cambridge, UK/New York:
583 Cambridge University Press.

584 Koutsodendris, A., Sachse, D., Appel, E., Herb, C., Fischer, T., Fang, X. & Pross, J.
585 (2018). Prolonged monsoonal moisture availability preconditioned glaciation of the
586 Tibetan Plateau during the Mid-Pleistocene Transition. *Geophysical Research*
587 *Letters*, 45(23), 13020-13030. doi:10.1029/2018GL079303

588 Kleiven, H. F., Jansen, E., Fronval, T., & Smith, T. M. (2002). Intensification of
589 Northern Hemisphere glaciations in the circum Atlantic region (3.5–2.4 Ma) – ice-
590 rafted detritus evidence. *Palaeogeography, Palaeoclimatology, Palaeoecology*,
591 *184*(3-4), 213-223. doi.org/10.1016/S0031-0182(01)00407-2

592 Lawrence, K. T., Herbert, T. D., Brown, C. M., Raymo, M. E., & Haywood, A. M.
593 (2009). High-amplitude variations in North Atlantic sea surface temperature during
594 the early Pliocene warm period. *Paleoceanography and Paleoclimatology*, *24*(2),
595 PA2218. doi:10.1029/2008PA001669

596 Licht, A., Dupont-Nivet, G., Pullen, A., Kapp, P., Abels, H. A., Lai, Z., Guo, Z., Abell,
597 J., & Giesler, D. (2016). Resilience of the Asian atmospheric circulation shown by
598 Paleogene dust provenance. *Nature communications*, *7*, 12390.
599 doi.org/10.1038/ncomms12390

600 Lisiecki, L. E., & Raymo, M. E. (2005). A Pliocene-Pleistocene stack of 57 globally
601 distributed benthic $\delta^{18}O$ records. *Paleoceanography, 20*(1), PA1003.
602 doi:10.1029/2004pa001071

603 Lu, H., Wang, X., & Li, L. (2010). Aeolian sediment evidence that global cooling has
604 driven late Cenozoic stepwise aridification in central Asia. *Geological Society,*
605 *London, Special Publications*, *342*(1), 29-44. doi.org/10.1144/SP342.4

606 Lu, Y., Fang, X., Appel, E., Wang, J., Herb, C., Han, W., Wu, F., & Song, C. (2015).
607 A 7.3–1.6 Ma grain size record of interaction between anticline uplift and climate
608 change in the western Qaidam Basin, NE Tibetan Plateau. *Sedimentary Geology,*
609 *319*, 40-51. doi:10.1016/j.sedgeo.2015.01.008

610 Luo, C., Zheng, Z., Tarasov, P., Pan, A., Huang, K., Beaudouin, C., & An, F. (2009).
611 Characteristics of the modern pollen distribution and their relationship to
612 vegetation in the Xinjiang region, northwestern China. *Review of Palaeobotany*
613 *and Palynology*, *153*(3-4), 282-295. doi:10.1016/j.revpalbo.2008.08.007

614 Ma, Q., Zhu, L., Wang, J., Ju, J., Lü, X., Wang, Y., Guo, Y., Yang, R., Kasper, T.,
615 Haberzettl, T., & Tang, L. (2017). *Artemisia*/Chenopodiaceae ratio from surface
616 lake sediments on the central and western Tibetan Plateau and its application.

*Palaeogeography, Palaeoclimatology, Palaeoecology*. doi:10.1016/j.palaeo.2017.05.002

Martínez-Botí, M. A., Foster, G. L., Chalk, T. B., Rohling, E. J., Sexton, P. F., Lunt, D. J., Pancost, R. D., Badegr, M. P. S., & Schmidt, D. N. (2015). Plio-Pleistocene climate sensitivity evaluated using high-resolution $CO_2$ records. *Nature*, *518*(7537), 49. doi.org/10.1038/nature14145

Miao, Y., Fang, X., Herrmann, M., Wu, F., Zhang, Y., & Liu, D. (2011a). Miocene pollen record of KC-1 core in the Qaidam Basin, NE Tibetan Plateau and implications for evolution of the East Asian monsoon. *Palaeogeography, Palaeoclimatology, Palaeoecology, 299*(1-2), 30-38. doi:10.1016/j.palaeo.2010.10.026

Miao, Y., Meng, Q., Fang, X., Yan, X., Wu, F., & Song, C. (2011b). Origin and development of *Artemisia* (Asteraceae) in Asia and its implications for the uplift history of the Tibetan Plateau: A review. *Quaternary International, 236*(1-2), 3-12. doi:10.1016/j.quaint.2010.08.014

Miao, Y., Fang, X., Liu, Y.-S., Yan, X., Li, S., & Xia, W. (2016). Late Cenozoic pollen concentration in the western Qaidam Basin, northern Tibetan Plateau, and its significance for paleoclimate and tectonics. *Review of Palaeobotany and Palynology, 231*, 14-22. doi:10.1016/j.revpalbo.2016.04.008

Molnar, P., Boos, W. R., & Battisti, D. S. (2010). Orographic Controls on Climate and Paleoclimate of Asia: Thermal and Mechanical Roles for the Tibetan Plateau. *Annual Review of Earth and Planetary Sciences, 38*(1), 77-102. doi:10.1146/annurev-earth-040809-152456

Naafs, B. D. A., Stein, R., Hefter, J., Khélifi, N., De Schepper, S., & Haug, G. H. (2010). Late Pliocene changes in the North Atlantic current. *Earth and Planetary Science Letters*, *298*(3), 434-442. doi.org/10.1016/j.epsl.2010.08.023

643 Naafs, B. D. A., Hefter, J., Acton, G., Haug, G. H., Martínez-Garcia, A., Pancost, R.,
644 & Stein, R. (2012). Strengthening of North American dust sources during the late
645 Pliocene (2.7 Ma). *Earth and Planetary Science Letters, 317-318*, 8-19.
646 doi:10.1016/j.epsl.2011.11.026

647 Naish, T. R., & Wilson, G. S. (2009). Constraints on the amplitude of Mid-Pliocene
648 (3.6–2.4 Ma) eustatic sea-level fluctuations from the New Zealand shallow-marine
649 sediment record. *Philosophical Transactions of the Royal Society of London A:*
650 *Mathematical, Physical and Engineering Sciences*, *367*(1886), 169-187.
651 doi:10.1098/rsta.2008.0223

652 Rea, D. K., Snoeckx, H., & Joseph, L. H. (1998). Late Cenozoic eolian deposition in
653 the North Pacific: Asian drying, Tibetan uplift, and cooling of the northern
654 hemisphere. *Paleoceanography, 13*(3), 215-224.

655 Sun, Y., An, Z., Clemens, S. C., Bloemendal, J., & Vandenberghe, J. (2010). Seven
656 million years of wind and precipitation variability on the Chinese Loess Plateau.
657 *Earth and Planetary Science Letters, 297*(3-4), 525-535.
658 doi:10.1016/j.epsl.2010.07.004

659 Van Campo, E., & Gasse, F. (1993). Pollen-and diatom-inferred climatic and
660 hydrological changes in Sumxi Co Basin (Western Tibet) since 13,000 yr BP.
661 *Quaternary Research*, *39*(3), 300-313. doi.org/10.1006/qres.1993.1037

662 Walter, H., Box, E. O. (1983). *The deserts of central Asia.* In M. Evenari, I. Noy-Meir
663 & D. W. Goodall (Eds.), *Ecosystems of the World* (Vol. 12A, pp. 193-236)*,*
664 Amsterdam: Elsevier Science Publishers.

665 Wang, W.M. (2004). On the origin and development of *Artemisia* (Asteraceae) in the
666 geological past. *Botanical Journal of the Linnean Society*, *145*(3), 331-336.
667 doi.org/10.1111/j.1095-8339.2004.00287.x

668 Wang, J., Wang, Y. J., Liu, Z. C., Li, J. Q., & Xi, P. (1999). Cenozoic environmental
669 evolution of the Qaidam Basin and its implications for the uplift of the Tibetan
670 Plateau and the drying of central Asia. *Palaeogeography, Palaeoclimatology,*
671 *Palaeoecology, 152*(1-2), 37-47. doi.org/10.1016/S0031-0182(99)00038-3

672 Wang, L., Lü, H. Y., Wu, N. Q., Li, J., Pei, Y. P., Tong, G. B., & Peng, S. Z. (2006).
673 Palynological evidence for Late Miocene–Pliocene vegetation evolution recorded
674 in the red clay sequence of the central Chinese Loess Plateau and implication for
675 palaeoenvironmental change. *Palaeogeography, Palaeoclimatology,*
676 *Palaeoecology*, *241*(1), 118-128. doi.org/10.1016/j.palaeo.2006.06.012

677 Wang, C., Zhao, X., Liu, Z., Lippert, P. C., Graham, S. A., Coe, R. S., Yi, H., Zhu, L.,
678 Liu, S., & Li, Y. (2008). Constraints on the early uplift history of the Tibetan
679 Plateau. *Proceedings of the National Academy of Sciences*, *105*(13), 4987-4992.
680 doi/10.1073/pnas.0703595105

681 Wang, J., Fang, X., Appel, E., & Song, C. (2012). Pliocene-Pleistocene climate
682 change at the NE Tibetan Plateau deduced from lithofacies variation in the drill
683 core SG-1, Western Qaidam Basin, China. *Journal of Sedimentary Research,*
684 *82*(12), 933-952. doi:10.2110/jsr.2012.76

685 Wei, H.-C., Ma, H.-Z., Zheng, Z., Pan, A.-D., & Huang, K.-Y. (2011). Modern pollen
686 assemblages of surface samples and their relationships to vegetation and climate
687 in the northeastern Qinghai-Tibetan Plateau, China. *Review of Palaeobotany and*
688 *Palynology, 163*(3-4), 237-246. doi:10.1016/j.revpalbo.2010.10.011

689 Yang, X., Scuderi, L., Paillou, P., Liu, Z., Li, H., & Ren, X. (2011). Quaternary
690 environmental changes in the drylands of China – A critical review. *Quaternary*
691 *Science Reviews, 30*(23-24), 3219-3233. doi:10.1016/j.quascirev.2011.08.009

692 Yin, A. (2010). Cenozoic tectonic evolution of Asia: A preliminary synthesis.
693 *Tectonophysics, 488*(1-4), 293-325. doi.org/10.1016/j.tecto.2009.06.002

694 Yuan, D. Y., Ge, W. P., Chen, Z. W., Li, C. Y., Wang, Z. C., Zhang, H. P., Zhang,
695 P.Z., Zheng, D. W., Zheng, W. J., Craddock, W. H., Dayem, K. E., Duvall, A. R.,
696 Hough, B. G., Lease, R. O., Champagnac, J. D., Burbank, D. W., Clark, M. K.,
697 Farley, K. A., Garzione, C. N., Kirby, E., Molnar, P., & Dayem, K. E. (2013). The
698 growth of northeastern Tibet and its relevance to large-scale continental
699 geodynamics: A review of recent studies. *Tectonics*, *32*(5), 1358-1370.
700 doi.org/10.1002/tect.20081

701 Zhang, P., Molnar, P., & Downs, W. R. (2001). Increased sedimentation rates and
702 grain sizes 2–4 Myr ago due to the influence of climate change on erosion rates.
703 *Nature*, *410*(6831), 891. doi.org/10.1038/35073504

704 Zhang, K., Zhao, Y., Yu, Z., & Zhou, A. (2010). A 2700-year high resolution pollen
705 record of climate change from varved Sugan Lake in the Qaidam Basin,
706 northeastern Tibetan Plateau. *Palaeogeography, Palaeoclimatology,*
707 *Palaeoecology, 297*(2), 290-298. doi:10.1016/j.palaeo.2010.08.008

708 Zhang, W., Appel, E., Fang, X., Song, C., & Cirpka, O. (2012a). Magnetostratigraphy
709 of deep drilling core SG-1 in the western Qaidam Basin (NE Tibetan Plateau) and
710 its tectonic implications. *Quaternary Research, 78*(1), 139-148.
711 doi:10.1016/j.yqres.2012.03.011

712 Zhang, W., Appel, E., Fang, X., Yan, M., Song, C., & Cao, L. (2012b). Paleoclimatic
713 implications of magnetic susceptibility in Late Pliocene–Quaternary sediments
714 from deep drilling core SG-1 in the western Qaidam Basin (NE Tibetan Plateau).
715 *Journal of Geophysical Research, 117*(B6). doi:10.1029/2011jb008949

716 Zhang, W., Appel, E., Fang, X., Song, C., Setzer, F., Herb, C., & Yan, M. (2014).
717 Magnetostratigraphy of drill-core SG-1b in the western Qaidam Basin (NE Tibetan
718 Plateau) and tectonic implications. *Geophysical Journal International, 197*(1), 90-
719 118. doi:10.1093/gji/ggt439

720 Zhao, Y., & Herzschuh, U. (2009). Modern pollen representation of source vegetation
721 in the Qaidam Basin and surrounding mountains, north-eastern Tibetan Plateau.
722 *Vegetation History and Archaeobotany, 18*(3), 245-260. doi:10.1007/s00334-008-
723 0201-7

724 Zhao, Y., Yu, Z., Chen, F., Ito, E., & Zhao, C. (2007). Holocene vegetation and
725 climate history at Hurleg Lake in the Qaidam Basin, northwest China. *Review of*
726 *Palaeobotany and Palynology, 145*(3-4), 275-288. doi:
727 10.1016/j.revpalbo.2006.12.002

728 Zhao, Y., Yu, Z., Chen, F., Zhang, J., & Yang, B. (2009). Vegetation response to
729 Holocene climate change in monsoon-influenced region of China. *Earth-Science*
730 *Reviews, 97*(1-4), 242-256. doi:10.1016/j.earscirev.2009.10.007

731 Zhao, Y., Yu, Z., Liu, X., Zhao, C., Chen, F., & Zhang, K. (2010). Late Holocene
732 vegetation and climate oscillations in the Qaidam Basin of the northeastern
733 Tibetan Plateau. *Quaternary Research, 73*(1), 59-69.
734 doi:10.1016/j.yqres.2008.11.007

735 Zhao, Y., Liu, H., Li, F., Huang, X., Sun, J., Zhao, W., Herzschuh, U., Tang, Y.
736 (2012). Application and limitations of the *Artemisia*/Chenopodiaceae pollen ratio in
737 arid and semi-arid China. *The Holocene, 22*, 1385-1392.
738 doi:10.1177/0959683612449762

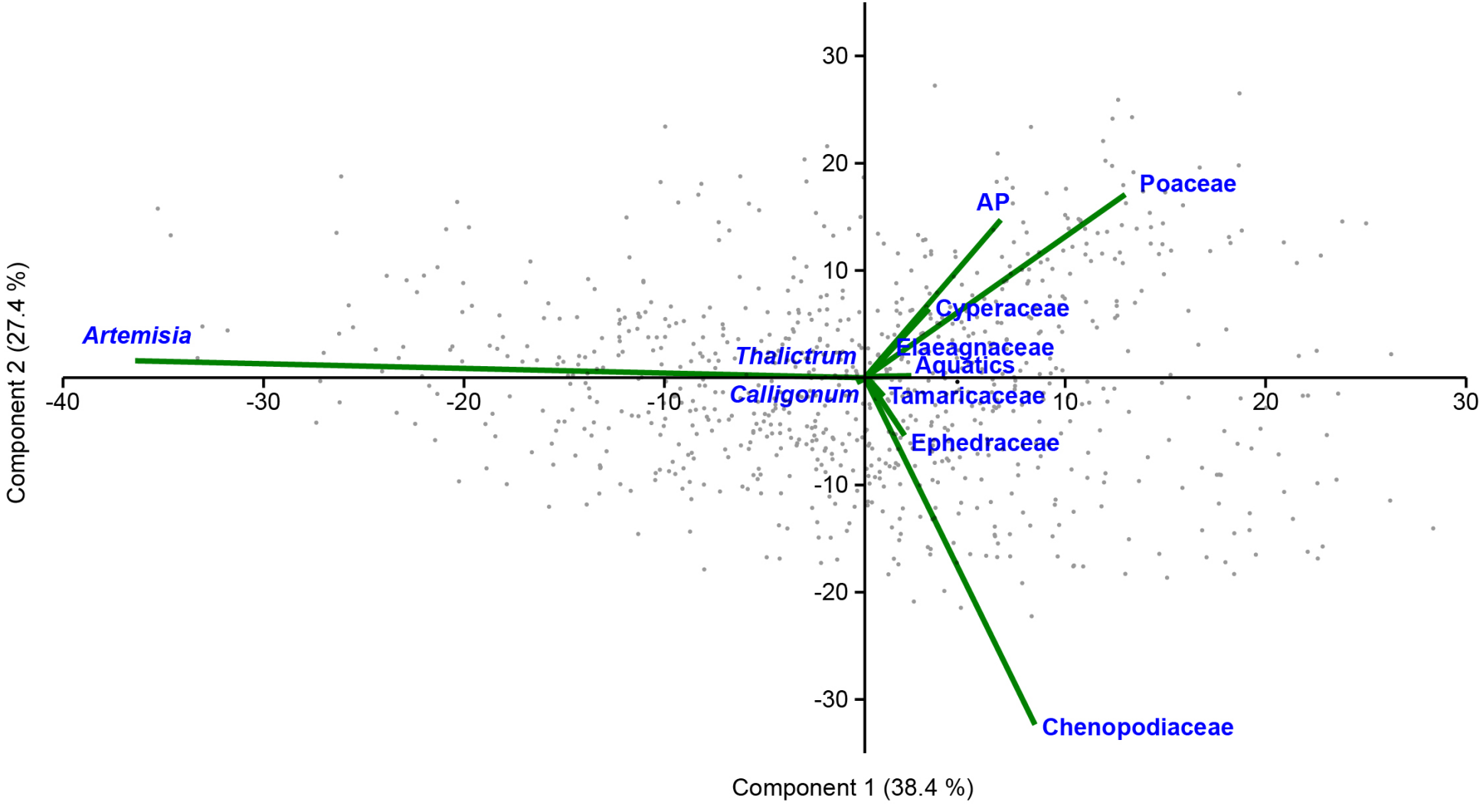
Component 2 (27.4 %)
Component 1 (38.4 %)
30
20
10
-10
-20
-30
-40
-30
-20
-10
10
20
30
Artemisia
Thalictrum
Calligonum
AP
Poaceae
Cyperaceae
Elaeagnaceae
Aquatics
Tamaricaceae
Ephedraceae
Chenopodiaceae